

Manganese induces mitochondrial dynamics impairment and apoptotic cell death: A study in human Gli36 cells



Agustina Alaimo^{a,1}, Roxana M. Gorodjod^{a,1}, Esteban A. Miglietta^a, Alejandro Villarreal^b, Alberto J. Ramos^b, Mónica L. Kotler^{a,*}

^a Departamento de Química Biológica, Facultad de Ciencias Exactas y Naturales, Universidad de Buenos Aires, IQUIBICEN-CONICET, Buenos Aires, Argentina

^b Instituto de Biología Celular y Neurociencias Prof. E. De Robertis, Facultad de Medicina, Universidad de Buenos Aires, Buenos Aires, Argentina

HIGHLIGHTS

- Gli36 glioma cells strongly express the astrocytic markers GFAP and S100B.
- Mn cytotoxicity triggers a caspase-dependent mitochondrial apoptotic pathway.
- Mn induces alterations in Opa-1, Mfn-2 and Drp-1 expression levels.
- Mn impairs the mitochondrial dynamics in human astrocyte-like cells.

ARTICLE INFO

Article history:

Received 6 August 2013

Received in revised form 26 August 2013

Accepted 27 August 2013

Keywords:

Apoptosis
Astrocytes
Human Gli36 cell line
Manganese toxicity
Manganism
Mitochondrial dynamics

ABSTRACT

Manganese (Mn) is an essential trace element due to its participation in many physiological processes. However, overexposure to this metal leads to a neurological disorder known as Manganism whose clinical manifestations and molecular mechanisms resemble Parkinson's disease. Several lines of evidence implicate astrocytes as an early target of Mn neurotoxicity being the mitochondria the most affected organelles. The aim of this study was to investigate the possible mitochondrial dynamics alterations in Mn-exposed human astrocytes. Therefore, we employed Gli36 cells which express the astrocytic markers GFAP and S100B. We demonstrated that Mn triggers the mitochondrial apoptotic pathway revealed by increased Bax/Bcl-2 ratio, by the loss of mitochondrial membrane potential and by caspase-9 activation. This apoptotic program may be in turn responsible of caspase-3/7 activation, PARP-1 cleavage, chromatin condensation and fragmentation. In addition, we determined that Mn induces deregulation in mitochondria-shaping proteins (Opa-1, Mfn-2 and Drp-1) expression levels in parallel with the disruption of the mitochondrial network toward to an exacerbated fragmentation. Since mitochondrial dynamics is altered in several neurodegenerative diseases, these proteins could become future targets to be considered in Manganism treatment.

© 2013 Elsevier Ireland Ltd. All rights reserved.

1. Introduction

Chronic exposure to high levels of inhalable Manganese (Mn) causes a neurodegenerative disease termed Manganism. This disorder is characterized by severe psychiatric and extrapyramidal motor dysfunctions that closely resemble Idiopathic Parkinson disease [23]. Manganism is considered primarily as an occupational disease. Mn is used in pesticides, animal feed, alkaline batteries and colorants for bricks. Furthermore, this metal may

also be introduced into the environment through emissions from steel plants, mining operations and the burning of fuel containing MMT (methylcyclopentadienyl manganese tricarbonyl), an additive and octane enhancer in some gasoline mixtures [10].

Manganism is characterized by the accumulation of high levels of Mn in the basal ganglia [3,23]. Particularly, the *globus pallidus* is considered the brain region initially affected by Mn exposure in which GABAergic neurons represent the primary target of damage [23].

Astrocytes are dynamic and metabolically active cells that accumulate Mn through a high affinity transport system. Consequently, they play a key role in Manganism development and progress [5,28]. Once it is imported into the cell, Mn is principally sequestered by the mitochondria through the Ca^{2+} uniporters [4] which represent the main site of damage [1,11].

* Corresponding author at: Int. Güiraldes 2160, Ciudad Universitaria, C1428EGA Buenos Aires, Argentina. Tel.: +54 1145763342; fax: +54 1145763342.

E-mail addresses: moniquekotler@gmail.com, kotler@qb.fcen.uba.ar (M.L. Kotler).

¹ Both authors made equal contribution to this work.

Notwithstanding conventional images showed mitochondria as static organelles, they are organized as an interconnected dynamic network. This is the consequence of a delicate balance between fusion and fission events that control the mitochondrial morphology and movement. Fusion and fission processes govern multiple functions such as mtDNA stability, respiratory capacity, response to cellular stress, mitophagy and apoptosis through a battery of mitochondria-shaping proteins [8,15]. In addition, when the intrinsic apoptotic pathway is triggered, mitochondria undergo prominent structural changes including exacerbated fission and cristae remodeling that ultimately mobilize the major pool of cytochrome c to the cytosol [8].

Several reports indicate that Mn induces apoptosis in different cell types mainly by triggering the mitochondrial pathway [1,11,18,20,27]. However, the underlying molecular mechanisms implicated in Mn-induced apoptosis in glial cells have been poorly elucidated in human cells. Furthermore, in this context there is no evidence that the intrinsic pathway is involved and whether fusion and fission equilibrium is impaired in Mn neurotoxicity. The aim of this study was to explore the possible mitochondrial dynamics alterations in Mn-exposed Gli36 cells, a cell line derived from a human glial tumor. In the present report, we described for the first time the occurrence of mitochondrial dynamics imbalance in Mn-exposed human astrocytes undergoing apoptosis.

2. Materials and methods

2.1. Cell culture and treatment

Human glioma Gli36 cells were maintained in DMEM (Sigma) supplemented with 10% heat-inactivated FBS (Fetal Bovine Serum) (BIO-NOS; Argentina), 2.0 mM glutamine, 100 units/ml penicillin, 100 µg/ml streptomycin and 2.5 µg/ml amphotericin B. After culture at 37 °C and 5% CO₂–95% air to yield 70–80% confluence, cells were exposed to MnCl₂ (Sigma) for 24 h.

2.2. MTT assay

Cell viability was assessed by 3-(4,5-dimethyl-thiazol-2-yl)-2,5-diphenyl-tetrazolium bromide (MTT) (Sigma) reduction assay as previously described [17] with slight modifications [1].

2.3. Neutral Red assay

The Neutral Red (NR) dye (Sigma) accumulates in lysosomes of viable uninjured cells. This technique was performed according to [6] with slight modifications [1].

2.4. Apoptotic nuclei detection

Evaluation of apoptotic nuclei was performed according to [1] using Hoechst 33258 (1 µg/ml) (Sigma). Images were analyzed with an Nikon Eclipse E800 C1 (Nikon Instech Co.) equipped with objective lens Nikon Plan Apo 100X/1.40 Oil, DAPI (λ_{ex} : 330–380 nm; λ_{em} : 435–485 nm). Digital pictures were analyzed and assembled using ImageJ software (NIH). Uniformly stained nuclei were scored as healthy cells (normal), whereas apoptotic cells were scored evaluating the presence of condensed and fragmented nuclei.

2.5. Caspase-3/7 activity assay

After Mn exposure, cells were washed with PBS and specific activity was measured as described in Ref. [11] employing the substrate Ac-DEVD-pNA. Results were expressed as pNA absorbance

units per mg protein. Protein concentration was determined according to Ref. [7].

2.6. Western blotting

Western blots were performed according to procedure previously described [11]. Antibodies: PARP-1 (H-250), Bax (N-20), Bcl-2 (N-19), Mfn-2 (H-68), anti-β-Actin (C4), rabbit IgG-HRP and mouse IgG-HRP (Santa Cruz Biotechnology); Opa-1 (612607) and Drp-1 (611113) (BD Pharmingen). Each membrane was reprobed with an anti-β-actin to normalize for protein loading. Immunoreactive bands were detected by chemiluminescence employing ECL detection reagents (Sigma) and analyzed using the LAS 1000 plus Image Analyzer (Fuji). Quantitative changes in protein levels were evaluated with ImageJ software (NIH).

2.7. Analysis of mitochondrial membrane potential ($\Delta\varphi_m$) and morphology

Cells were exposed to MitoTracker Red CMXRos (Molecular Probes) fluorescent probe for 30 min at 37 °C. Then, cells were washed with PBS and fixed with 4% PFA. Finally, samples were examined under a FV300 confocal fluorescence microscope (Olympus Corp.) (λ_{ex} : 543 nm) equipped with an image acquisition system and Fluoview 3.3 software (Olympus Corp.). Digital pictures were analyzed and assembled using ImageJ software (NIH).

2.8. Immunocytochemistry

Cells were fixed with 4% PFA, permeabilized with 0.25% Triton X-100-PBS (10 min, RT) washed with PBS and incubated in 1% BSA-PBS for 30 min at RT. Cells were incubated with primary antibodies anti-GFAP (Glial Fibrillary Acid Protein) (1:3000) (DAKO) and anti-S100B (S100 calcium binding protein B) (1:1000) (Sigma) for 24 h at 4 °C. The specific staining was detected with secondary antibodies conjugated with FITC or Rhodamine RRX (1:800) (Jackson ImmunoResearch). Negative controls were performed under the same conditions without primary antibodies (data not shown). Samples were examined under a fluorescence microscope Olympus IX-81 (Olympus Corp.). Digital pictures were analyzed and assembled using Adobe Photoshop 7.0 software and ImageJ software (NIH).

2.9. Statistics

Experiments were carried out in triplicate unless otherwise stated. Results are expressed as mean ± SEM values. Experimental comparisons between treatments were made by Student's *t*-test or one-way ANOVA followed by Student–Newman–Keuls *post hoc* test with statistical significance set at *p* < 0.05. All analyses were carried out with GraphPad Prism 4 software (GraphPad Software).

3. Results

3.1. Human Gli36 cells express astrocytic markers

Gli36 cells growing in monolayer exhibit a flat and mainly stellated morphology (Fig. 1A). The immunocytochemical analysis showed that both GFAP and S100B (extensively used as markers for astrocytes identification [24]) are expressed in Gli36 cells confirming their astrocytic lineage (Fig. 1B).

3.2. Mn-induced cytotoxicity

To investigate the Mn cytotoxic effects, we exposed cells to increasing concentrations of MnCl₂ (200–1000 µM) for 24 h. The

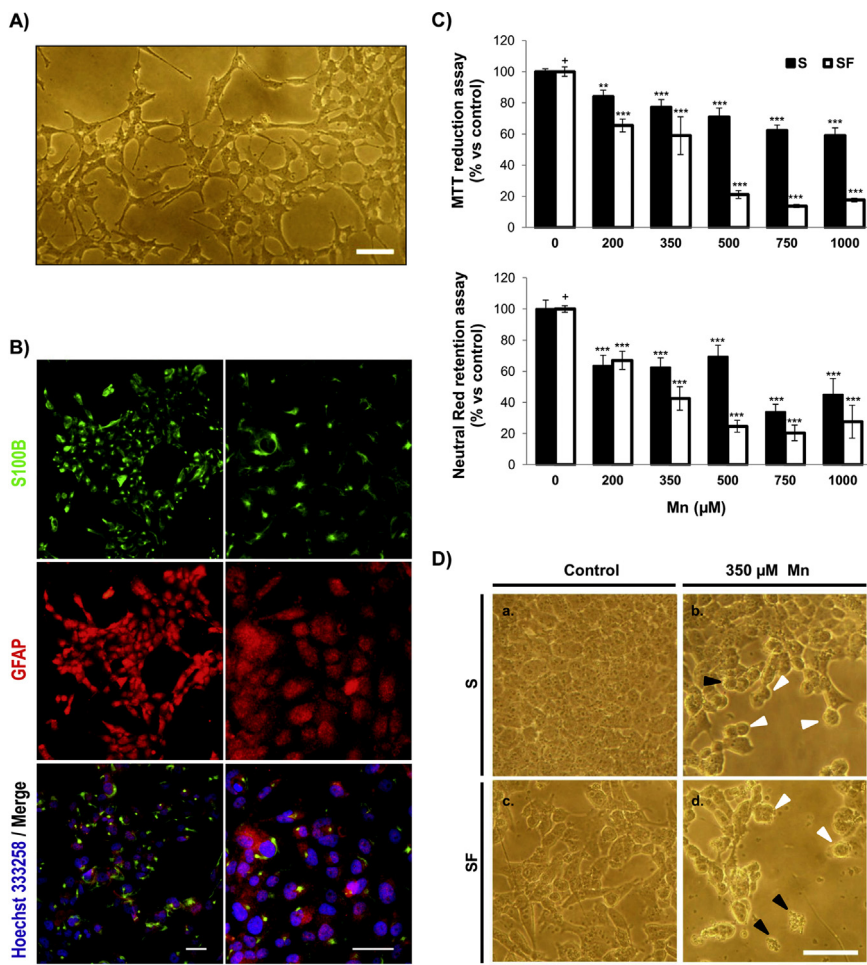


Fig. 1. (A) Gli36 morphological features. Phase-contrast image of cells growing under culture. (B) Immunocytochemistry of astrocytic markers: GFAP and S100B. Magnification: 10× (left panels) and 20× (right panels). (C) Mn-induced cytotoxicity. Viability assayed by MTT and NR. Data were expressed as average ± SEM ($n=8$) and controls were considered 100%. ** $p<0.01$, *** $p<0.001$ vs. respective control. * $p<0.05$ vs. control S (SF: MTT: $82.4 \pm 3.1\%$; NR: $79 \pm 2.1\%$). (D) Phase-contrast microscopy. Cells exposed to 350 μM Mn displayed cell monolayer disruption with shrinkage and retraction of cellular processes (white arrowheads) and membrane blebbing (black arrowheads). Arrows show representative events through the samples. Scale bar: 50 μm.

incubation time was selected from the cell viability vs. incubation time curve (data not shown).

It has been reported that the use of serum has substantial disadvantages such as protection from metal toxicity [14,22]. Hence, we performed experiments in serum (S) and serum free (SF) media. Results indicated that Mn induces concentration-dependent cytotoxicity (Fig. 1C). Particularly, 350 μM Mn generated a moderate cell death (~40–50%) measured by both MTT and NR methods. Morphological characteristics consistent with apoptosis such as rounded, shrunken and loosely attached cells with plasma membrane blebbing were observed (Fig. 1D). These events were more pronounced in SF conditions. In addition, serum deprivation by itself induced ~20% decrease in cell viability. Therefore, we employed 350 μM Mn in further experiments to evaluate the events implicated in Mn-induced cell death.

3.3. Mn triggers apoptotic cell death

Caspase-3 plays a critical role in the apoptotic cascade being PARP-1 (poly [ADP-ribose] polymerase-1) one of its main targets. Cleavage of PARP-1 in fragments of 89 and 24 kDa is considered an apoptotic marker [9]. Therefore, to determine the possible participation of an apoptotic caspase-dependent pathway, we assessed caspase 3/7 activity and examined PARP-1 levels by western blot analysis. Our results showed that Mn induces an increase of $63 \pm 2\%$ ($p<0.01$) and $68 \pm 12\%$ ($p<0.001$) in caspase-3/7 activity

in S and SF conditions, respectively (Fig. 2A). Correspondingly, we found a decrease in PARP-1 full length protein levels (116 kDa) with an almost complete signal disappearance in SF conditions (Fig. 2B). Chromatin condensation and nuclear fragmentation are morphological hallmarks of apoptosis. We observed an increase in condensed and fragmented nuclei in parallel with a marked decrease in the number of cells, being these events more pronounced in SF conditions (Fig. 2C, b and d). Overall, our results demonstrate that Mn induces a caspase-dependent apoptotic cell death in Gli36 cells.

3.4. The mitochondrial apoptotic pathway is involved in Mn-induced apoptosis

The mitochondrial apoptotic pathway is triggered by alterations in mitochondrial structure and function, including mitochondrial membrane permeabilization (MMP) and release of pro-apoptotic factors into the cytosol, such as cytochrome c. This hemeprotein together with Apoptotic Protease Activating Factor-1, dATP/ATP and caspase-9 form the apoptosome, a multi-protein complex that activates this initiator caspase. Besides, the MMP is controlled by a balance between the pro- and anti-apoptotic members of the Bcl-2 family [12,26]. To evaluate the intrinsic apoptotic pathway involvement in our model, we first monitored the activation of caspase-9 by pre-incubating cells with the specific inhibitor (Ac-LEHD-CMK, 10 μM, Calbiochem). As shown in Fig. 2D this inhibitor

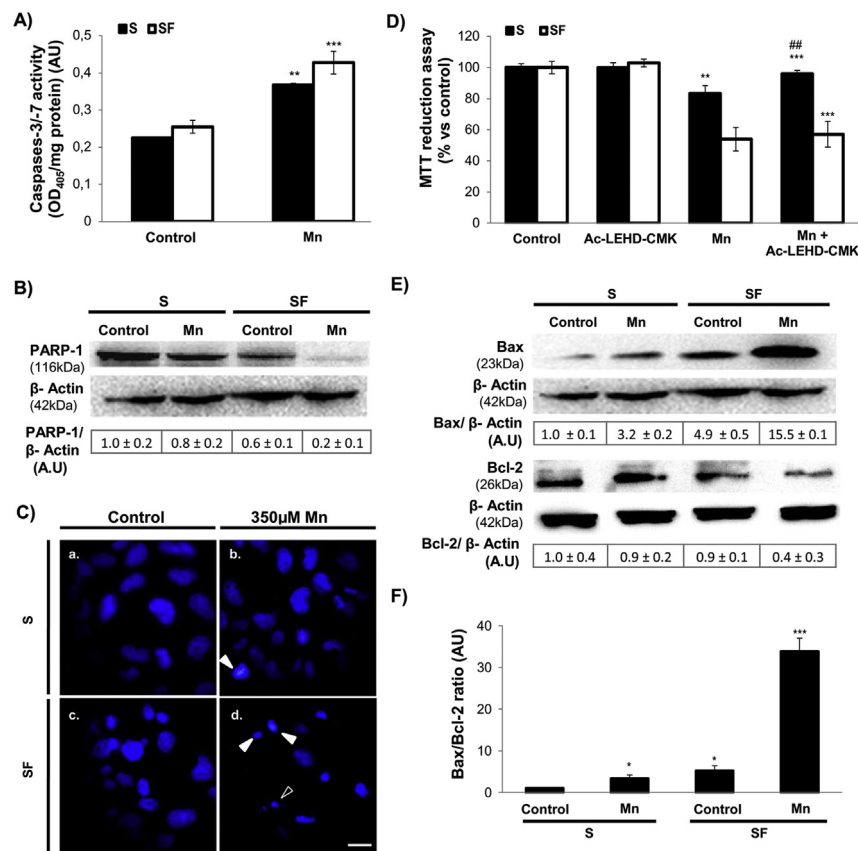


Fig. 2. Mn triggers apoptotic cell death. Cells were incubated for 24 h with 350 μ M Mn under S or SF conditions. (A) Caspase 3/7 activity. Specific activity was determined spectrophotometrically using a specific substrate Ac-DEVD-pNA (100 μ M). (B) PARP-1 cleavage. (C) Apoptotic nuclei. Hoechst 33258 staining showed the presence of nuclear condensation (filled arrowheads) or fragmentation events (open arrowhead). Arrows show representative events through the samples. (D) Caspase-9 activation. Pre-incubation with Ac-LEHD-CMK (10 μ M, 1 h) was evaluated by MTT assay. Data were expressed as average \pm SEM ($n = 8$) and controls were considered 100%. (E) Bax and Bcl-2 expression levels. (F) Bax/Bcl-2 ratio was calculated based on Western Blot signals quantified with the ImageJ software. * $p < 0.05$, ** $p < 0.01$, *** $p < 0.001$ vs. respective control and # $p < 0.01$ vs. Mn under S conditions. AU: arbitrary units. Scale bar: 10 μ m.

prevented cell death ($p < 0.01$) only under S conditions. Thereafter, we determined the ratio between the pro-apoptotic Bax protein and its anti-apoptotic counterpart Bcl-2. Western blot analysis of cell lysates revealed that Mn increases Bax levels (3.2- and 15.5-fold under S and SF conditions respectively) while decreases Bcl-2 expression (~50%) under SF conditions. As a consequence, Bax/Bcl-2 ratio is enhanced (34-fold; $p < 0.001$) favoring the susceptibility toward cell death (Fig. 2E and F). Finally, we evaluated the $\Delta\varphi_m$ dissipation employing MitoTracker Red CMXRos. Results showed that Mn induced the $\Delta\varphi_m$ collapse evidenced by the presence of high dye fluorescence in the cytoplasm, being more pronounced in SF conditions (Fig. 3A, see arrows). Collectively, these results suggest that the apoptotic intrinsic pathway is involved in Mn-induced cell death in Gli36 cells.

3.5. Mn impairs the mitochondrial dynamics

Mitochondria are highly dynamic organelles that can fuse and divide during cell life. These morphologies are controlled by a tight balance between two antagonistic events: fusion and fission [8,15]. A morphological analysis of cells loaded with MitoTracker Red CMXRos (Fig. 3A) revealed the occurrence of a mitochondrial network disruption induced by Mn. In fact, control cells under S conditions displayed elongated, thread-like mitochondria while Mn-treated cells, as well as those serum deprived, exhibited smaller punctuated mitochondria, suggesting an imbalance between fusion and fission processes toward the latter. Notably, the effect of Mn under SF conditions resulted to be extremely severe. In this case cell morphology was totally lost indicating a complete damage over

mitochondrial mass. To gain further insight into the events related with mitochondrial dynamics, we focused on key mitochondria-shaping proteins. Since Opa-1 (Optic atrophy protein-1) and Mfn-2 (Mitofusin-2) are required for mitochondrial membrane fusion and Drp-1 (Dynamin related protein-1) is considered the master regulator of mitochondrial fission [8], we studied their expression levels in Mn-exposed cells. As shown in Fig. 3B–D, Mn induced a decrease in Opa-1 and Mfn-2 expression ($p < 0.01$) whereas Drp-1 levels were markedly increased ($p < 0.001$). No significantly differences were observed in the expression levels of mitochondria-shaping proteins under SF conditions. Altogether, these findings suggest that Mn induced an imbalance in the fusion–fission equilibrium in Gli36 cells (Fig. 3E).

4. Discussion

In the present report, we examined morphological and immunocytochemical characteristics of the Gli36 cell line derived from a human glial tumor. Their tumorigenic properties have been demonstrated since the s.c. injection of cultured cells into nude mice gave rise to growing tumors [2]. Despite being extensively used as a viral host, to our knowledge, these cells were not immunocytochemically characterized. The morphological evaluation showed that Gli36 cells resemble normal human astrocytes and other human glioblastoma cell lines [29]. In the present report, most Gli36 cells were strongly positive for both GFAP and S100B (Fig. 1A and B) thus confirming their astrocytic origin.

We next analyzed the effect of Mn exposure on cell viability. Experiments were carried out both in the presence and the

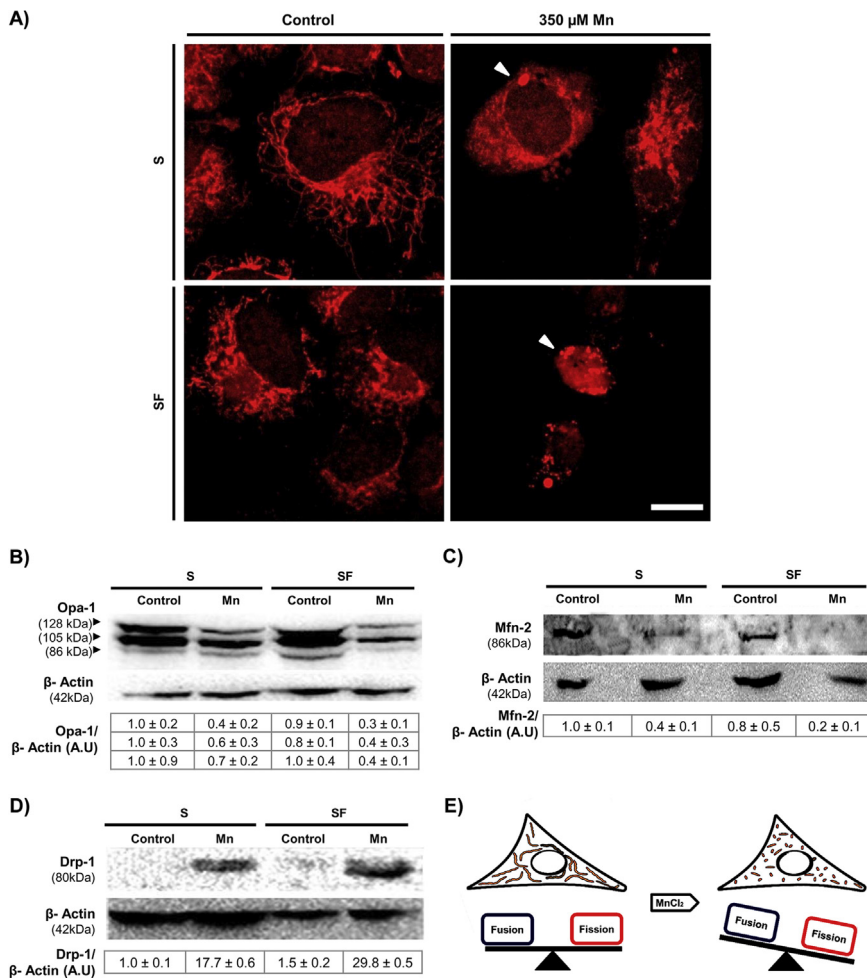


Fig. 3. $\Delta\varphi_m$ dissipation and mitochondrial dynamics alterations. (A) Mitochondria were labeled with 75 nM MitoTracker Red CMXRos and visualized by laser confocal microscopy. Scale bar: 10 μm . Arrows show cells presenting $\Delta\varphi_m$ disruption and are representative events through the samples. (B)–(D) Western blot analysis of mitochondria-shaping proteins expression levels: Opa-1, Mfn-2 and Drp-1. (E) Scheme illustrating the effect of Mn on fusion–fission equilibrium in Gli36 cells.

absence of FBS. Similar results were obtained in both scenarios with cytotoxicity being more severe in SF conditions. Although serum is widely used in cell culture to improve *in vitro* growth, its employment in certain situations results detrimental [22]. It has been reported that serum protects cells from toxicity induced by several transition metals. Particularly, Mn can bind transferrin, α_2 -macroglobulin and albumin being the latter the prevalent protein in mammalian sera and the potential cause for the reduction of metal-induced cytotoxicity [21]. Moreover, cells in the central nervous system are protected by the blood–brain barrier which maintains a much more restricted *milieu* than culture media containing 10% FBS [22]. Our results demonstrated that Gli36 cells resulted sensitive to Mn in both the presence and absence of serum (Fig. 1C and D).

Several reports have proposed that Mn cytotoxicity is mainly associated with mitochondrial dysfunction and the trigger of the intrinsic/mitochondrial apoptotic pathway [1,12,18,20,27]. Our findings demonstrated that 350 μM Mn induced an increase in Bax/Bcl-2 ratio, $\Delta\varphi_m$ loss and caspase-9 activation (Figs. 2D–F and 3A). To the best of our knowledge, this is the first report describing the Mn-induced mitochondrial impairment in human astrocyte-like cells. Surprisingly, Ac-LEHD-CMK was unable to prevent Mn-induced cell death under SF conditions. Under these critical circumstances we should contemplate the impossibility to prevent cells from dying. However, we cannot dismiss the

chance that the inhibitor concentration tested may have been low. However, higher concentrations of Ac-LEHD-CMK resulted toxic for cells (data not shown).

Mitochondrial apoptotic pathway may be in turn responsible for the subsequent events described such as caspases-3/-7 activation, chromatin condensation and fragmentation (Fig. 2A–C), membrane blebbing and cell shrinkage (Fig. 1D). All these events support the involvement of an apoptotic pathway triggered by Mn. As far as we know, only two reports have studied the apoptotic effect of Mn in human glial cells. One of them distinguish TUNEL positive U-87 MG cells after Mn exposure (1 mM, 72 h) [20] and the other detected caspase-3 activation and chromatin condensation and fragmentation for 100–800 μM , 24 h in T98G cells [18]. In the present study we described more comprehensively the different steps involved in Mn-induced apoptosis in Gli36 cells. Precisely, our results indicate that Mn activates a caspase-dependent mitochondrial apoptotic pathway.

Mitochondria typically form a non-static reticular network regulated through a complex equilibrium between fission and fusion processes. The balance between these events is controlled by multiple proteins that mediate the outer and inner mitochondrial membranes remodeling [8]. As far as we know, there are no previous reports describing the mitochondrial dynamics in Mn-treated human cells undergoing apoptosis. In this report we demonstrate for the first time that Mn induces a shift in fusion–fission balance

resulting in a mitochondrial network fragmentation enhancement in human astrocytes. This phenomenon is the consequence of decreased Opa-1 and Mfn-2 and increased Drp-1 expression levels (Fig. 3A–D). Interestingly, the fission event contributes to mitochondria quality control by enabling the autophagic removal of damaged organelles (mitophagy) and can facilitate apoptosis [30]. Based on this evidence we cannot rule out the possibility that this process could be implicated in our model. In this scenario, cells under SF conditions (an autophagic inductor) would be more vulnerable to Mn than their counterparts with serum. Experiments supporting this hypothesis are in progress in our laboratory (data not shown).

Increasing evidence suggest that defects in mitochondrial dynamics correlate with the progression of neurodegenerative diseases such Alzheimer's, Huntington's and Parkinson's [25]. The present study provides novel evidence to consider Manganism as another neurodegenerative disorder in which mitochondrial dynamics is impaired.

As mentioned above, serum deprivation resulted in a 20% decrease in cell viability. Even though we detected a 5-fold increment in Bax/Bcl-2 ratio under these conditions, most of the apoptotic events induced by Mn were absent: (a) cells did not exhibit the morphological appearance typically observed in this process (Fig. 1D), (b) neither caspase-9 nor caspase-3/-7 were activated (Fig. 2A and D), (c) $\Delta\phi m$ remained intact (Fig. 3A). Surprisingly, PARP-1 levels were decreased in SF conditions in comparison with S (Fig. 2B). This enhanced cleavage may be mediated by other proteases different from caspases [9]. Based on these results we speculated that although mitochondria could be slightly dysfunctional, SF conditions *per se* did not trigger a caspase-dependent apoptotic pathway.

It has been reported that serum deprivation could induce the cell cycle arrest in G₀ [13]. Moreover, it was demonstrated that mitochondrial morphology and their biogenesis are integrated to the cell cycle [19]. In particular, mitochondria of G₀ arrested NRK cells exhibited mostly intermediate and fragmented morphologies [16]. Notably, we observed these mitochondrial events in serum deprived Gli36 cells although no changes in the mitochondria-shaping proteins expression levels were observed (Fig. 3). Therefore, we cannot reject the hypothesis that these cells undergo growth arrest under starvation.

5. Conclusions

Our results demonstrated that Mn induces caspase-dependent apoptotic cell death in human Gli36 cells. In this report we described for first time the impairment in the fusion–fission balance in Mn toxicity. Since mitochondrial dynamics is altered in several neurodegenerative diseases, Opa-1, Mfn-2 and Drp-1 could become future targets to be considered in Manganism treatment.

Conflict of interest

The authors declare that there are no conflicts of interest.

Acknowledgments

This work was supported by Consejo Nacional de Investigaciones Científicas y Técnicas, CONICET (PIP 0356). The authors acknowledge Dr. Osvaldo Uchitel for providing Gli36 cells and Roberto Fernandez for his assistance in obtaining confocal microscopy images (FBMC-FCEN-UBA, IFIBYNE-CONICET, Argentina). The authors thank Dr. Cecilia Poderoso (Departamento Química Biológica, FMED, UBA, INBIOMED-CONICET, Argentina) for

providing Mfn-2 antibody. A.A, R.M.G. and A.V. thank CONICET and E.A.M. thanks CIN for the studentships. A.J.R. and M.L.K. are research members of CONICET.

References

- [1] A. Alaimo, R.M. Gorjod, M.L. Kotler, The extrinsic and intrinsic apoptotic pathways are involved in manganese toxicity in rat astrocytoma C6 cells, *Neurochem. Int.* 59 (2011) 297–308.
- [2] E. Arwert, S. Hingtgen, J.L. Figueiredo, H. Bergquist, U. Mahmood, R. Weissleder, K. Shah, Visualizing the dynamics of EGFR activity and antglioma therapies *in vivo*, *Cancer Res.* 67 (2007) 7335–7342.
- [3] M. Aschner, Manganese: brain transport and emerging research needs, *Environ. Health Perspect.* 108 (2000) 429–432.
- [4] M. Aschner, M. Gannon, H.K. Kimelberg, Manganese uptake and efflux in cultured rat astrocytes, *J. Neurochem.* 58 (1992) 730–735.
- [5] M. Aschner, T.R. Guijarro, J.S. Schneider, W. Zheng, Manganese: recent advances in understanding its transport and neurotoxicity, *Toxicol. Appl. Pharmacol.* 221 (2007) 131–147.
- [6] E. Borenfreund, J.A. Puerner, Toxicity determined *in vitro* by morphological alterations and neutral red absorption, *Toxicol. Lett.* 24 (1985) 119–124.
- [7] M.M. Bradford, A rapid and sensitive method for the quantitation of microgram quantities of protein utilizing the principle of protein-dye binding, *Anal. Biochem.* 72 (1976) 248–254.
- [8] S. Campello, L. Scorrano, Mitochondrial shape changes: orchestrating cell pathophysiology, *EMBO Rep.* 11 (2010) 678–684.
- [9] G.V. Chaitanya, A.J. Steven, P.P. Babu, PARP-1 cleavage fragments: signatures of cell-death proteases in neurodegeneration, *Cell Commun. Signal.* 8 (2010) 31.
- [10] H. Checkoway, Documenting neurotoxicity from occupational manganese exposure, *Occup. Environ. Med.* 67 (2010) 362–363.
- [11] L.E. Gonzalez, A.A. Juknat, A.J. Venosa, N. Verrengia, M.L. Kotler, Manganese activates the mitochondrial apoptotic pathway in rat astrocytes by modulating the expression of proteins of the Bcl-2 family, *Neurochem. Int.* 53 (2008) 408–415.
- [12] A. Jourdain, J.-C. Martinou, Mitochondrial outer-membrane permeabilization and remodelling in apoptosis, *Int. J. Biochem. Cell Biol.* 41 (2009) 1884–1889.
- [13] T.J. Langan, R.C. Chou, Synchronization of mammalian cell cultures by serum deprivation, *Methods Mol. Biol.* 761 (2011) 75–83.
- [14] L.M. Latinwo, V.L. Badisa, C.O. Odewumi, C.O. Ikediobi, R.B. Badisa, A. Brooks-Walter, A.T. Lambert, J. Nwoga, Comparative evaluation of cytotoxicity of cadmium in rat liver cells cultured in serum-containing medium and commercially available serum-free medium, *Int. J. Mol. Med.* 22 (2008) 89–94.
- [15] M. Liesa, M. Palacín, A. Zorzano, Mitochondrial dynamics in mammalian health and disease, *Physiol. Rev.* 89 (2009) 799–845.
- [16] K. Mitra, C. Wunder, B. Roysam, G. Lin, J. Lippincott-Schwartz, A hyperperfused mitochondrial state achieved at G1–S regulates cyclin E buildup and entry into S phase, *Proc. Natl. Acad. Sci. U.S.A.* 106 (2009) 11960–11965.
- [17] T. Mosmann, Rapid colorimetric assay for cellular growth and survival: application to proliferation and cytotoxicity assays, *J. Immunol. Methods* 65 (1983) 55–63.
- [18] E.-J. Park, K. Park, Induction of oxidative stress and inflammatory cytokines by manganese chloride in cultured T98G cells, human brain glioblastoma cell line, *Toxicol. In Vitro* 24 (2010) 472–479.
- [19] Y.-Y. Park, H. Cho, Mitofusin 1 is degraded at G2/M phase through ubiquitylation by MARCH5, *Cell Div.* 7 (2012) 25.
- [20] S. Puli, J.C.K. Lai, K.L. Edgley, C.K. Daniels, A. Bhushan, Signaling pathways mediating manganese-induced toxicity in human glioblastoma cells (U87), *Neurochem. Res.* 31 (2006) 1211–1218.
- [21] O. Rabin, L. Hegedus, J.M. Bourre, Q.R. Smith, Rapid brain uptake of manganese(II) across the blood–brain barrier, *J. Neurochem.* 61 (1993) 509–517.
- [22] H.J. Romijn, Development and advantages of serum-free, chemically defined nutrient media for culturing of nerve tissue, *Biol. Cell* 63 (1988) 263–268.
- [23] J.A. Roth, Are there common biochemical and molecular mechanisms controlling manganism and parkinsonism, *Neuromol. Med.* 11 (2009) 281–296.
- [24] M.V. Sofroniew, H.V. Vinters, Astrocytes: biology and pathology, *Acta Neuropathol.* 119 (2010) 7–35.
- [25] B. Su, X. Wang, L. Zheng, G. Perry, M.A. Smith, X. Zhu, Abnormal mitochondrial dynamics and neurodegenerative diseases, *Biochim. Biophys. Acta* 1802 (2010) 135–142.
- [26] S.W.G. Tait, D.R. Green, Mitochondria and cell death: outer membrane permeabilization and beyond, *Nat. Rev. Mol. Cell Biol.* 11 (2010) 621–632.
- [27] C. Tamm, F. Sabri, S. Ceccatelli, Mitochondrial-mediated apoptosis in neural stem cells exposed to manganese, *Toxicol. Sci.* 101 (2008) 310–320.
- [28] E. Tiffany-Castiglioni, Y. Qian, Astroglia as metal depots: molecular mechanisms for metal accumulation, storage and release, *Neurotoxicology* 22 (2001) 577–592.
- [29] G. Wollmann, M.D. Robek, A.N. van den Pol, Variable deficiencies in the interferon response enhance susceptibility to vesicular stomatitis virus oncolytic actions in glioblastoma cells but not in normal human glial cells, *J. Virol.* 81 (2007) 1479–1491.
- [30] R.J. Youle, A.M. van der Bliek, Mitochondrial fission, fusion, and stress, *Science* 337 (2012) 1062–1065.